Laser Assisted Micro Grinding of Titanium

Ashish Kumar Sahu (ashkumar17@gmail.com)
Indian institute of technology delhi https://orcid.org/0000-0002-8803-9051
Sunil Jha

Research Article

Keywords: hybrid machining, laser structuring, micro grinding, surface morphology

Posted Date: November 12th, 2021

DOI: https://doi.org/10.21203/rs.3.rs-968496/v1

Abstract

Laser assisted micro-grinding (LAMG) is an emerging area of research in the field of high-quality micro-job fabrication and performance improvement. Conventional micro grinding (CMG) by micro pencil grinding tool suffers drawbacks such as tool deflection, higher cutting force and poor surface finish. In the present work, authors have attempted to investigate the performance of LAMG and CMG in the fabrication of micro-channel on Titanium material. Surface of workpiece was structured with the help of air assisted nanosecond-pulsed fiber laser scanning prior to the CMG at the different values of laser power by keeping scanning velocity constant. During the study, the CMG forces were recorded and after the processes surface roughness of the fabricated microchannels was measured. Results have shown reduction in the magnitude of the normal and tangential force by 31 % and 44 %, respectively, in LAMG compared to the CMG. In addition to that better surface finish was observed in LAMG than CMG. The surface roughness of micro-channel and grinding forces were found to be dependent on the power density of laser. Increase in the laser power deteriorates the surface finish and reduces the magnitude of grinding forces. High grinding forces in the CMG led to the dynamic deflection of the grinding wheel which produced the vibration in the process. The excessive vibration in CMG processes exploited the surface finish of the micro-channel. Such vibration was not observed on the LAMG process; as a result, better dimensional accuracy and surface finish of the channel was found.

1. Introduction

High precision micro parts and surfaces help to bridge the gap between the macro and nanoscale. Microstructure fabrication of hard metallic parts is challenging due to their higher strength and increasing demands of micro components [1]. Non-mechanical micro-manufacturing methods, similar to lithography and Electro Discharge Machining (EDM), are generally costly and tedious. They are likewise simply pertinent to some particular kind of conductive materials. Hence, the micro structuring of hard materials is usually accomplished by diamond grinding tools at higher cutting speeds [2, 5]. In microchannel fabrication, materials with high hardness face conventional microgrinding (CMG) problems due to high tool wear, higher grinding forces, and tool vibrations. As a result, the grinding cost is very high and ranges from 60–80% of the component cost [3]. In any case, further examination is needed to advance the profitability, device expenses, and quality norms of the method to build its application.

The microgrinding technique is widely employed to fabricate microchannels. Titanium and its alloy are an enthusiastically suggested material for biomedical and aviation applications. Diamond grain peeled off from the tool because of the high resistance of the material and lower electroplate bonding strength due to the higher hardness property of Titanium. Peeled off grains may embed with the machined surface and reduces the surface finish [1, 15, 16].

Several researchers tried to analyze the different attributes of the CMG process in past studies. Kadivir et al. performed CMG of Titanium. The effect of depth of cut, cutting speed tool feed, and dressing ratio on grinding force and surface roughness were analyzed [1]. Lee et al. optimized the process parameters in

CMG for normal force, tangential force and surface roughness, considering the depth of cut, feed rate and air temperature as a parameter on tool steel [2]. In another investigation, the surface integrity of the micro-ground surface of titanium alloy was studied using different cutting velocities and feed rate to depth ratios [4]. Gong et al. fabricated a microchannel on Ti-6Al-4V by F800 grain particle size. Surface finish up to 0.325μm was achieved on a high spindle speed of 60,000 rpm and a low feed rate of 20μm/s [5]. Cheng et al. concluded that higher grain size W40 was best for Ti-6Al-4V micro-surface grinding based on lesser tool wear and lodging. Compared to the continuous tool, cutting forces were decreased by 35–40% when utilizing a discontinuous tool [6]. Arrabiyeh et al. fabricated a micro pencil grinding tool of 50μm diameter and performed microchannel fabrication on 16MnCr5 hardened steel. The results showed that an increase in cutting speed and tilt angle improves the quality of machined structures and improves the tool life. Increasing the grit size of the abrasive increases the tool life significantly [7]. Ren et al. investigated the effect of grain size on CMG of silicon with the micro pencil grinding tool (MPGT)I. Increased grit size lower down the finish and increases the average edge chipping width. Effect of spindle speed, tool feed and depth of cut were analyzed on surface roughness and average edge chipping width. [8]

Laser assisted grinding was performed to improve the efficiency of CMG by softening of material prior to grinding. Kumar et al. observed 43.25% reductions in cutting forces in laser assisted grinding (LAG) with lesser tool wear in the machining of silicon nitride ceramic. Thermal cracks were induced by laser prior to CMG, which removes more volume of material.[3]. Sheng et al. performed laser thermal shock-assisted zirconia grinding and observed the reduction in cutting force and specific grinding energy. The brittleness of zirconia gets increased after laser irradiation, which reduces the cutting forces [9]. Kizaki et al. simulated the temperature in LAG of zirconia by micro-diamond burr and observed improved surface morphology [11]. Azarhoushang et al. investigated laser micro structuring of silicon nitride ceramics on single grit grinding. Lateral crack increases with laser assistance, which reduces specific grinding energy while grinding, which increases the quality of ground surfaces [10]. Ma et al. have shown that the LAG archives ductile regime grinding of zirconia with a larger depth of cut and lesser roughness. Conventional grinding has a lateral crack on the surface; however, the LAG surface has no cracks [12].

In another study, Azarhoushang concluded that finding suitable laser energy controls the depth of laser-induced damage and the grinding depth. Higher energy could deteriorate the surface [13]. Researchers also tried grinding tool structuring for better process efficiency. Butler et al. compared Ti-6Al-4V micro grinding using the electroplated tool and laser-ablated patterned CVD diamond tool. It was observed that work material adhesion took place on both the tools, but the laser-patterned tool retained its cutting edges, whereas the electroplated tool was completely clogged and found to be incapable of cutting in the form of chips. Chip flow becomes easier in laser-structured tool. Lesser surface roughness was observed in laser structured CVD tool [17]. Another study by Kadivar et al. analyzed the effect of tool structuring and workpiece structuring on normal force, tangential force and surface roughness on Si_3N_4. They concluded the 10% of tool structuring is more effective than workpiece structuring; however, surface roughness increased by structuring. Tool life is also improved with tool structuring [13].

Hybrid grinding techniques such as laser assisted microgrinding (LAMG) reduce the cutting force and improve tool life. The LAG is based on the local time softening of the workpiece material. Preheating of material soften it, which is removed by grinding tool with lesser forces and lower tool wear. Preheating of material leads to reduced material strength and stiffness, which softens the material along the cutting path [12]. The drawback behind the process is that the process is only applicable without coolant. However, the temperature generated in micro grinding is very high.

The CMG process with micro pencil grinding tool (MPGT) faces several challenges like high grinding force, higher specific grinding energy (SGE), and tool vibrations [1, 16]. LAG with the MPGT tool was not reported in previous studies. This paper describes a novel approach of hybrid micro grinding methods with a micro pencil grinding tool. In this study, the effect of tool feed and cutting speed is analyzed on forces and surface roughness in CMG [1, 18]. In LAMG, the workpieces structuring was performed by ns laser machining assisted with air to structure the workpiece; afterwards, micro grinding was performed using a pencil grinding tool to remove the structured surface. The laser structuring effect was investigated on the microchannel surface quality and cutting forces with different laser power levels. The process was compared with conventional micro grinding for developed cutting forces and surface roughness. Further, the effect of laser input energy density was investigated on cutting forces and surface roughness. In the last section, the surface morphology of sequential LAMG and CMG ground surfaces are compared.

2. Materials And Methods

Experimental machining system

The LAMG is performed on Advance Micromachining System (AMMS), a multi-process 5-axes CNC micromachining system developed in-lab at IIT Delhi [14]. Various conventional and non-conventional processes like micro milling, micro grinding, micro-drilling, micro-LBM, and micro EDM are available in a single machining setup to fabricate micro components by different methods. This CNC system has an axes precision of 1 µm and vibration-free granite structure [16].

A nanosecond fiber laser (SPI G4 EP-Z 50W) with a Precitec cutting head is employed to structure the workpiece on AMMS. Laser pulses of the nanosecond regime could achieve higher fluence for melting and vaporization of the substrate. Laser source specifications are mentioned in table 1. The laser beam is focussed on top of the surface, maintaining a constant gap of 0.2 mm between the nozzle and workpiece top surface at the focal condition.

ss

Table 1 Fiber Laser Source Specifications

Collimated beam Dia	Beam quality (M^2)	Max. pulse energy	Wavelength	Focussed beam dia (d)	Nozzle orifice
15mm	1.6	1mJ	1060nm	7.2µm	0.5mm

A high-speed aerostatic bearing spindle of Nakanishi (NRAF 5080 with E3000 controller) is available on AMMS to perform high speed conventional micro grinding. The spindle rotation speed is max up to 80,000 RPM with runout within 1µm. The aerostatic spindle has a 3mm collet to hold the grinding tool to perform microgrinding. In the sequential machining initially, the surface is machined with laser machining assisted with air. So, the workpiece surface is structured with laser heating followed by micro pencil grinding tool machining.

Hybrid grinding methods and parameters

In the hybrid grinding method, CMG and laser structuring are combined to fabricate the microchannel. In the fabrication method, the workpiece surface is structured with laser, and the structured surface is ground with an MPGT. The laser structuring process is assisted with pressurized air to avoid recast and repositioning of melted material. The laser structure dimension is lesser than the grinding tool dimension, so laser heating does not affect the surface surrounding to channel. The laser structuring position is such that it should be at the centre of the grinding tool path. The schematics of the process of hybrid grinding is shown in figure 1(a). Figure 1(b) shows the method on AMMS to perform laser structuring followed by tool grinding. Both the processes were performed on the same machine tool to avoid repositioning errors. Machining on the same machine ensures the direction and orientation of the channel.

Laser scan strategy

CMG requires high specific energy to ground material with abrasives at high cutting velocity. A very high temperature is generated due to the high rotational speed of the tool. So, to reduce the specific energy consumption laser assisted grinding methodology is utilized. The substrate surface is structured by laser energy in LAMG. The transferred laser energy melts and vaporizes the material, which gets expulse away by pressured air. In the experimentation, two patterns of laser structuring were utilized, as shown in Figure 2. The laser structure dimension is lesser than the tool dimension so that the structured surface can be ground with the grinding tool in a single pass in the width direction of the workpiece. The laser beam scan the material in structuring prior to grinding at 60mm/s at 1mJ of pulse energy with varying pulse repletion rate (PRR) 15-30kHz. Pattern 2 has a higher laser energy density than pattern 1 as the longitudinal width is decreased from 0.3mm to 0.2mm, increasing the energy density per unit area. As the energy density increases, the melting and vaporization phenomena increased. The portion of material removed increases with increases in energy density. The structuring process develops cracks on the surface beneath the removed material. So the specific energy consumption in the removal of material gets reduced in LAMG to remove the surface.

Grinding tool and workpiece

A electroplated micro pencil diamond grinding tool (Nakanishi code 12005, dia500µm) is suitable for non-ferrous material, i.e., titanium grade 2 (Cp-Ti). Micro pencil grinding tool (MPGT) has 3mm of shank diameter with 2mm of burr length and 320 grit size. The grinding tool specification is shown in table 2. The microchannel of 4mm length was fabricated on the sample (size 20mm(*l*)×10mm(*w*)× 5mm (*d*)) [7]. The workpiece is cut into the required dimension by wire EDM and prepared before fabrication by polishing. Fine grade sandpaper followed by cloth polishing is utilized for the finishing of sample substrate before channel fabrication.

Table 2 Micro grinding tool specification Nakanishi diamond burr 12005[19]

Dia	Diamond size	Grit size	Shank dia	Total length	Abrasive type	Type	Burr Length
0.5mm	29.5µm	320	3mm	38mm	diamond	Electroplated	2mm

Experimentation

Experimentation starts with the effect of grinding feed and cutting speed on cutting forces and surface roughness of microchannel. Further, Sequential LAMG is performed to analyze the impact of laser structuring on micro grinding. The experiments were performed at different laser power to investigate the effect on the normal force, tangential force, and surface roughness. Areal roughness is analyzed in terms of average surface roughness S_a and root mean square roughness S_q. Similarly, in the next section, the impact of laser scan density was analyzed and compared with CMG in two patterns of laser scanning. The parameters of grinding and laser structuring are shown in table 3.

Table 3 Hybrid machining parameters

Parameters	**Value**
Workpiece material	Titanium Grade 2
Laser structuring parameters	Pulse energy(E)1mJ, PRR 15-30kHz, laser power P_L=15-30W, laser scan velocity v_l= 60mm/s, Pulse width t_{pulse}=250ns
Micro grinding tool	Dia.500µm, Nakanishi12005
CMG Parameters	feed (*f*)1-5mm/min, cutting speed (v_s) 35-125mm/min, depth of cut (a_p) 5-20µm

3. Result And Discussion

3.1 Laser structuring effect

Laser structuring removes material and develops cracks on the surface of the substrate. The portion of material removed by laser structuring in ablation gets increased with an increase in laser power. The laser heats the material lattice and raises the temperature, leading to the expulsion of material by melting and vaporization. The temperature generated by nanosecond pulses is in the range of melting and sublimate the structured material. The transformation of melted material is rapid, so the material transforms in the gaseous state, and the melted material is removed by pressurized air. Varying laser power will influence the dimension and geometry of the structured surface. Power will increase the depth of removal of melted material and affect the ablation mechanism and the structure's surface dimension.

Figure 3 demonstrate the geometry and dimension of the laser structure. The pressurized air helps to remove the melted material from the structured surface, so the geometry created varies with the increase in laser power energy. The absorbed energy is increasing with an increase in power. The transferred energy develops cracks on the surface, damaging the material surface and loosening the metal bonds by local excitation of atoms by laser structuring. Increasing the laser structure dimension and energy density will increase the thermal damage and increases the cracks in depth. The laser structured surface has increased density of cracks with an increase in absorbed energy. The increasing density of laser structures increases the thermal damage on the workpiece surface and inferior surface quality, which increases the roughness. The areal laser input energy density is expressed as Eq. 1[16]

$$E_{l-input} = \frac{E_L}{A_L} = \frac{P_L . t}{l_L w_L} \qquad (1)$$

where E_L is the total laser energy, and A_L is the total structured area, l_L is laser length scan and w_L is the width of laser scan. The total material removed in LAMG includes the material removed in laser structuring and CMG. The portion removed in laser structuring is comparatively lesser than CMG. Thus, laser structuring will reduce the cutting forces and specific grinding energy in the hybrid process.

3.2 Effect of tool feed and cutting speed on CMG performance

Initially the experiments were performed to analyze the effect of cutting speed and tool feed on CMG performance. The effect of tool feed can be seen in figure 4 on the normal force and tangential force in the micro end grinding process. Experiments were performed at 80mm/min cutting speed, and 5µm depth of cut and grinding tool feed varied between 1-5mm/min. The normal cutting force F_z was observed between 0.22N to 0.85N. The normal cutting forces increased with an increase in the tool feed due to an increase in undeformed chip thickness. Undeformed chip thickness ( ) during micro-slot grinding can be expressed as Eq. 2.[17]

$$h_m = M_d 2L \frac{f}{v_s} \quad (2)$$

Here M_d is a component variable to describe the effects when grinding enters microscale, *f is* tool feed, v_s is cutting speed, L is the distance between two adjacent grits, d_s is the tool diameter.

Similarly, Tangential force F_t can be calculated as Eq 3 where H is hardness, and K_c workpiece fracture toughness k is related to physical-mechanical properties, and ε and γ are parameters that can be determined based on the workpiece properties and grinding parameters [15].

$$F_t = \left(k \frac{H^3}{K_c^2} \gamma h_m^{2(1-\varepsilon)} \right) \quad (3)$$

Increasing uncut chip thickness increases the tangential force F_y as per equation 3, which is evident in figure 4(b). An increase in tool feed increases undeformed chip thickness, which increases the tangential force. Another observation from microchannel quality can be seen as the tool feed increases the dimensional accuracy of microchannel lower down due to tool vibration. Cantilever nature of the MPGT cause instability in grinding, which increases grinding force.

Increasing tool feed increases the roughness due to increased material per grain of removal, which increases surface roughness, as shown in figure 4(c). Another observation with the increase in tool feed is that the tool vibration increases. Due to higher tool rotation and high grinding feed increases tool radial vibration, which decreases the microchannel quality and dimensional accuracy. The channel profile is uneven at high tool feed which increases the roughness of the channel surface. Another reason for higher roughness could be the rubbing of the cantilevered nature of MPGT. In CMG, due to higher vibration, the tool becomes unstable during rotation. Unstable tool rotation is cause of rubbing instead of machining, which deteriorates the quality of the channel.

The effect of cutting speed is analyzed at *f*=1mm/min, a_p=20μm with a varied cutting speed of 35-125mm/min. Tool rotation varied from 22-80kRPM to vary the cutting speed. The grinding tool wear is neglected for analyzing the responses as the experiments were conducted with the same tool.

The normal force and tangential decreased with grinding speed, as shown in figure 5(a). As the cutting speed increases, undeformed chip thickness decreases. Decreasing the amount of material removed per rotation decreases the cutting forces. Also, increasing the more no. of active grains in the machining zone reduces the maximum undeformed chip thickness based on Eq. (2). Metal removal per grain and undeformed chip thickness were reduced at high cutting speed. So, forces also get decreased with lesser undeformed chip thickness. In the material removal mechanism with high cutting speed, more grains are

involved per unit length of machining. Therefore, the active distance between two adjacent grain (L) decreased at higher tool rotation.

Cutting speed also decreases the roughness of the microchannel, as shown in figure 5(c) for both roughness parameters. Undeformed chip thickness h_m get decreased with cutting speed. So, the material removed per grain of rotation is reduced with a higher cutting speed. The radial motion error decreased with the increase of tool speed of the aerostatic spindle [22]. Higher spindle speed was conducive to reduce surface roughness and restrain the generation of edge chipping. High cutting velocity was preferred in practical micro-grinding.

3.3 Effect of laser structuring on cutting forces in micro grinding

The cutting forces are compared in CMG with pattern 1 to understand the laser structuring effect with varied power. The impact of laser structuring is analyzed at *f*=2mm/min, a_p=5µm at a cutting speed of 80mm/min. The laser power varied for structuring, and the effect of laser power on grinding forces were analyzed. The comparison is shown in figure 6 (a) and (b) for the normal and tangential force with varying laser power and CMG. As it can be seen, the grinding force on the laser structured surface is comparatively lower than CMG. In LAMG, the lateral cracks developed as shown by Azarhoushang et al. and lesser axial cracks, which reduces the cutting force [13]. Due to partial removal of material in the laser structuring surface, the material removal per grain decreases LAMG forces and specific energy consumption.

The effect of varying power shows that as the energy in laser structuring increases, the thermal damage increases, so the material melting is more and gets removed by air pressure. The normal force decreased with an increase in laser power. A similar trend can be seen with tangential force. A maximum reduction of 31% in normal force and 44% in tangential force were observed at 25W compared to CMG. Similarly, tangential force is also lesser compared to CMG. The material removal per grain is reduced due to partial material removal, which lower down the grinding forces.

3.4 Effect of laser structuring on surface roughness

The surface roughness was measured to find the impact of laser structuring on the surface quality of micro-ground channel. The comparison was demonstrated in terms of S_a and S_q with varying laser power and CMG channel bottom surface roughness. As can be seen from the LAMG method, the roughness is significantly reduced compared to CMG at lower power, as shown in figure 6(c). Surface roughness increases with an increase in laser power.

According to the result in CMG, the axial cracks developed, which cause higher roughness, as mentioned by Azarhoushang et al. [13]. Another reason could be a higher cutting force, as evident by the force graph. In CMG, the vibration caused by cutting force is the reason for higher roughness, which is evident in the SEM image by marks surrounding the channel, as shown in figure 9. Higher removal increases uncut chip thickness compared to LAMG, which is the cause of higher roughness.

In LAMG, the lateral cracks developed as demonstrated by Azarhoushang et al. and lesser axial cracks, reducing the cutting force [13]. The lower cutting force also reduces tool vibration, which is evident by narrower channel width. So, lower roughness could be achieved. However, melting and removal of material are higher by increasing laser power, directly affecting the roughness. At 30 W laser power, the depth of thermal damage and melted material is higher than the depth of the channel, so the roughness increases drastically. The phenomena is evident in SEM image in which the thermally damaged surface is not completely removed by tool grinding.

3.5 Effect of laser input energy density

Two laser scan patterns are compared at 15 W of laser power to analyze the effect of laser input energy density on cutting forces and roughness, As shown in figure 2. In pattern 1, the transferred energy density is lesser compared to pattern 2 because of the longer laser scan length for the same channel length.

A comparison of forces achieved in the tangential and normal directions is shown in figure 7 (a-b). Increasing laser input energy per unit area rises melting, and the cracks density increases in depth. So, the removal of material becomes easier. Increased energy density improves the portion of material removed by structuring, and thermal damage got increased. The normal and tangential cutting force both achieved lesser in pattern 2. Tangential force decreased by 10.3% in pattern 1 and 36% in pattern 2 compared to CMG. Similarly, normal force decreased by 20.5% in pattern 1 and 38% less for pattern 2.

The surface roughness of the channel is also compared for pattern 1 and 2 to analyze the effect of laser energy density, as shown in figure 7(c). It can be seen in pattern 1 the laser energy density is lesser, so the roughness achieved is lower. However, with pattern 2, the roughness is increased again due to the effect of laser heating. The higher energy density damage material surface more and increases roughness. In pattern 1, S_a and S_q decreased by 24% and 22%, respectively, compared to CMG. Roughness increases in pattern 2 by 11% and 14.6% for S_a and S_q, respectively, compared to CMG. So the optimum laser energy density is needed for a better finish and lesser cutting force. Higher laser energy density increases the roughness. It can be concluded the laser structuring pattern should be optimized to control energy density for lower cutting forces and higher surface finish.

3.6 Surface morphology analysis

Microchannel surface morphology was analyzed to understand the machining mechanism during material removal in LAMG and CMG. Zeiss EVO18 captures SEM micrograph for microchannel quality and surface morphology are shown in figures 8-10. LAMG ground surface scanned with laser pattern 1 and 2 is shown in figure 9 and 10, respectively. The laser parameter is kept constant during both patterns, i.e.,15W and v_l=60m/s. The microchannel surface is compared at CMG parameter v_s=80mm/min, f=2 mm/min and a_p=5µm.

The SEM micrograph can be seen in CMG as the wider channel achieved compared to LAMG. The broader interaction of the tool is due to the radial vibration of the MPGT tool. Tool vibration is more prone

in the machining zone of hard material and due to the extended length of MPGT. The tool rubbing marks are visible on both sides of the channel due to the cantilever nature MPGT tool. The unevenness of the surface is higher due to vibrations, which increases the surface roughness of the channel. Both sides of channel tool motion marks are evident, which confirms the tool vibration. Dimensional accuracy is observed lower in CMG due to tool vibrations.

In the LAMG, the channel width is comparatively lower than micro grinding due to lesser vibration. The force developed in the LAMG process is lesser, so a stable micro-grinding process can be seen without tool vibration. Initial marks of tool entry can be seen due to sudden material interaction, leading to vibration and radial errors in the spindle, as shown in Figures 9 and 10. After that tool become stable, so better channel quality is achieved.

The material affected by laser structuring is deposited on the side walls in the tool rotation direction. The marks of varying depth visible in layers show the increasing depth in subsequent passes of laser structured grinding surface in the SEM image in figure 9. The material can be seen thermally affected according to the laser scan path at the channel track centre. The thermally affected material is removed with tool motion; however, it is not removed in small chips because it becomes amorphous and porous. The removed material was deposited on sidewalls after the thermal effect. The surface morphology seen improved compared to CMG; however, the thermally affected surface of the laser beam can be seen clearly. The material affected by laser heat smeared on the sidewalls of the channel.

In the LAMG, the surface is affected by laser heating, so a heat-affected surface is visible on the surface of the microchannel, which shows the path of the laser track. The tool motion does not completely remove the heat-affected zone. Instead, it shows the depth of the heat-affected zone is greater than the channel depth as shown in fig 9.

Figure 10 shows the SEM image of the channel fabricated by pattern 2 of laser scanning and CMG. In pattern 2, the laser energy transferred per unit area is higher than pattern 1 due to the denser laser path. Similar to pattern 1, the channel's width is lesser than the CMG channel due to the tool's lesser radial vibration, which was concluded by SEM micrograph. However, roughness increases with laser energy density due to excessive thermal damage in depth compared to pattern 1. Thermal damage deteriorates surface and more significant HAZ due to longer interaction time. The affected material does not remove entirely by tool machining. On the surface, the removed material ablation marks can be seen at the corner of the scan track as there is a longer interaction due to the interpolation of axis motion between laser beam and material. The heat affected material grains were pulled out by the grinding tool. The portion of material removed is more by a laser beam, so lesser material needs to be removed per grain of tool motion, reducing the uncut chip thickness. So lesser force was achieved compared to pattern 1 and CMG. The optimization of laser power and energy density is required for a specific depth of the channel fabrication for the thermal structuring of the workpiece surface.

4. Conclusion

The proposed novel laser assisted grinding process, in which ns pulsed lasers for micro structuring assisted with air on the workpiece prior to the grinding process, showed significant improvement compared to the conventional micro-grinding process. The main findings of this study are summarised below.

- Increasing tool feed increases the uncut chip thickness, which increases the normal force and tangential force. Uncut chip thickness increases the surface roughness of the microchannel. Similarly, increasing tool rotation reduces the cutting force and improves surface finish due to lesser material removed per grain of abrasive.
- The volume of ablated material by laser structuring is mainly influenced by the laser power, which directly influences the ablation mechanism of melting and vaporization.
- The investigation concludes the laser-structuring lower down the tangential and normal forces in sequential grinding method. Another conclusion of the study is that increasing laser power increases surface roughness. So optimum level of laser power is needed for lesser cutting force and roughness.
- Laser scanning pattern 1 has lower roughness, and pattern 2 has lesser cutting forces. So, increasing the laser structure energy density reduces the cutting forces, but it increases the roughness of the ground surface. So optimum scan path is required for laser scanning.
- The tool vibration gets lesser with LAMG due to structured material. In CMG, the tool becomes unstable, so rubbing of the tool is visible in the SEM micrograph. The channel width is more in CMG due to tool radial vibrations and vibration marks on the side edges of the channels. In LAMG, the removed material is submerged on the sidewalls of the channel.

This study shows that laser assisted grinding improves the machining efficiency and surface condition compared to CMG. Therefore, an extension of current work could be investigated and optimize the different scanning patterns and micro-grinding parameters for better output.

Declarations

Acknowledgements

The author would like to acknowledge the financial support from the Department of Science and Technology, Govt of India, for conducting research.

Competing interests The authors declare no competing interests.

Availability of data and materials Not applicable.

Code availability Not applicable

Ethics approval and consent to participate Not applicable.

Consent for publication Not applicable.

Author's Contribution

Ashish Kumar Sahu: Conceptualization, methodology, investigation, formal analysis, and writing, methodology,

Sunil Jha:Conceptualization, resources, writing—review and editing, supervision, project administration, and funding acquisition.

References

1. Kadivar M (2018) Micro-grinding of titanium
2. 1. Lee PH, Chung H, Lee SW (2011) Optimization of micro-grinding process with compressed air using response surface methodology. Proc Inst Mech Eng Part B J Eng Manuf 225:2040–2050. https://doi.org/10.1177/0954405411398808
3. Kumar M, Melkote S, Lahoti G (2011) Laser-assisted microgrinding of ceramics. CIRP Ann - Manuf Technol 60:367–370. https://doi.org/10.1016/j.cirp.2011.03.121
4. Kadivar M, Azarhoushang B, Daneshi A, Krajnik P. (2020) Surface integrity in micro-grinding of Ti6Al4V considering the specific micro-grinding energy. Procedia CIRP ;87:13–8. https://doi.org/10.1016/j.procir.2020.02.069.
5. Gong YD, Wen XL, Cheng J, Yin GQ, Wang C. (2014) Experimental study on fabrication and evaluation of a micro-scale shaft grinding tool. J Mech Sci Technol ;28:1027–37. https://doi.org/10.1007/s12206-013-1176-6.
6. Wen X, Cheng J. (2019) Experimental study of a specially designed diamond micro discontinuous grinding tool. Int J Adv Manuf Technol ;102:3341–56. https://doi.org/10.1007/s00170-019-03333-w.
7. Arrabiyeh PA, Setti D, Basten S, Kirsch B, Aurich JC. (2019) Micro grinding 16MnCr5 hardened steel using micro pencil grinding tools with diameters ∼50 μm. CIRP J Manuf Sci Technol ;27:1–10. https://doi.org/10.1016/j.cirpj.2019.10.002.
8. Ren Y, Li C, Li W, Li M, Liu H. (2019) Study on micro-grinding quality in micro-grinding tool for single crystal silicon. J Manuf Process ;42:246–56. https://doi.org/10.1016/j.jmapro.2019.04.030.
9. Xu S, Yao Z, Cai H, Wang H. (2017) An experimental investigation of grinding force and energy in laser thermal shock-assisted grinding of zirconia ceramics. Int J Adv Manuf Technol ;91:3299–306. https://doi.org/10.1007/s00170-017-0013-y.
10. Azarhoushang B, Soltani B, Daneshi A. (2018) Study of the effects of laser micro structuring on grinding of silicon nitride ceramics. CIRP Ann ;67:329–32. https://doi.org/10.1016/j.cirp.2018.04.084.
11. Kizaki T, Ito Y, Tanabe S, Kim Y, Sugita N, Mitsuishi M. (2016) Laser-assisted Machining of Zirconia Ceramics using a Diamond Bur. Procedia CIRP;42:497–502.

https://doi.org/10.1016/j.procir.2016.02.239.

12. Ma Z, Wang Z, Wang X, Yu T. (2020) Effects of laser-assisted grinding on surface integrity of zirconia ceramic. Ceram Int ;46:921–9. https://doi.org/10.1016/j.ceramint.2019.09.051.
13. Azarhoushang B, Soltani B, Zahedi A. (2017) Laser-assisted grinding of silicon nitride by picosecond laser. Int J Adv Manuf Technol ;93:2517–29. https://doi.org/10.1007/s00170-017-0440-9
14. Sahu AK, Jha S. (2020) Microchannel fabrication and metallurgical characterization on titanium by nanosecond fiber laser micromilling. Mater Manuf Process ;00:1–12. https://doi.org/10.1080/10426914.2020.1718702.
15. Ren JX, Hua DA. (2011) Grinding principle. Beijing: Publishing House of Electronics Industry; 2011
16. Cheng J, Gong YD. (2014) Experimental study of surface generation and force modeling in micro-grinding of single crystal silicon considering crystallographic effects. Int J Mach Tools Manuf 2014;77:1–15. https://doi.org/10.1016/j.ijmachtools.2013.10.003.
17. Butler-Smith PW, Axinte DA, Daine M. (2012) Solid diamond micro-grinding tools: From innovative design and fabrication to preliminary performance evaluation in Ti-6Al-4V. Int J Mach Tools Manuf 2012;59:55–64. https://doi.org/10.1016/j.ijmachtools.2012.03.003.
18. Kadivar M, Shamray S, Soltani B, Daneshi A, Azarhoushang B. (2019)La ser-assisted micro-grinding of Si3N4. Precis Eng ;60:394–404. https://doi.org/10.1016/j.precisioneng.2019.09.004.
19. S. Diameter, Symbols used in NAKANISHI Tools Catalogue Precautions for using Nakanishi Tools For safe use of the tools, (n.d.).

Figures

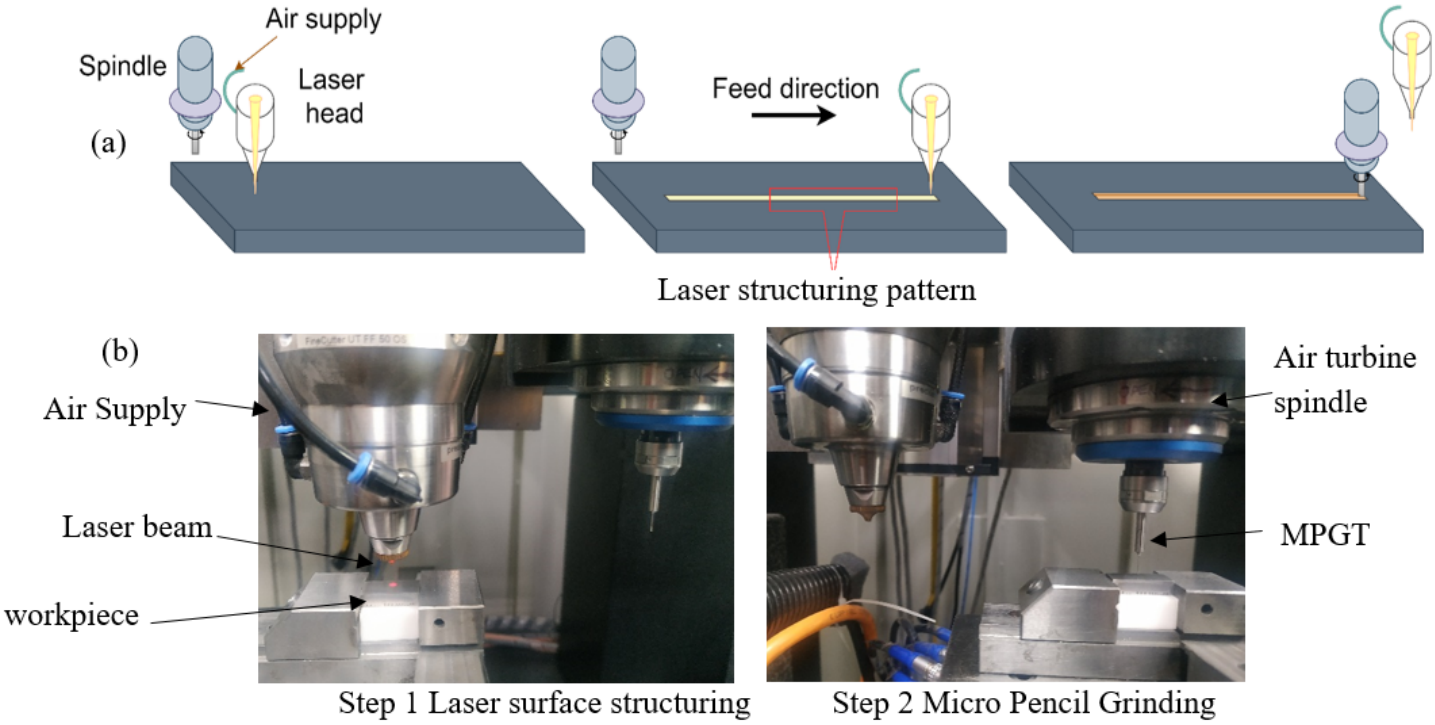

Figure 1

(a) Hybrid grinding process and laser path(b) Experiment steps

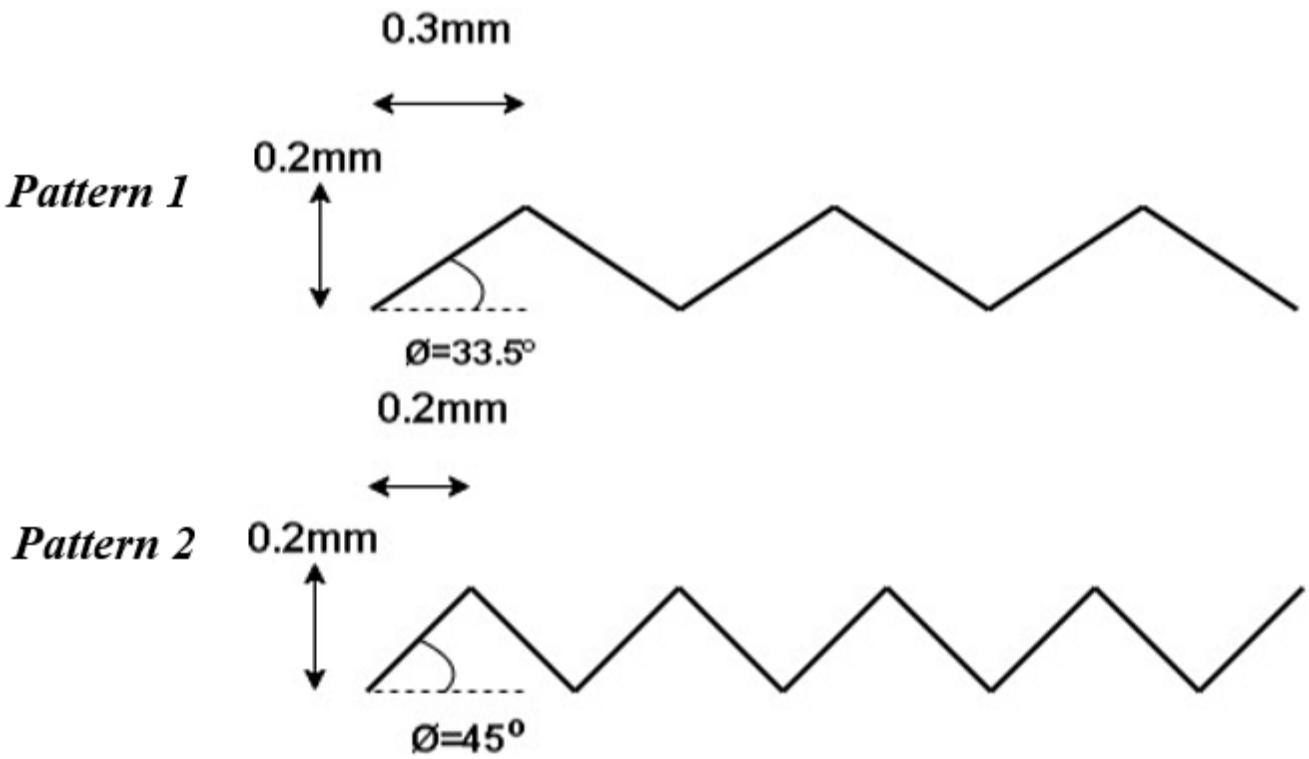

Figure 2

laser scan pattern for laser structuring

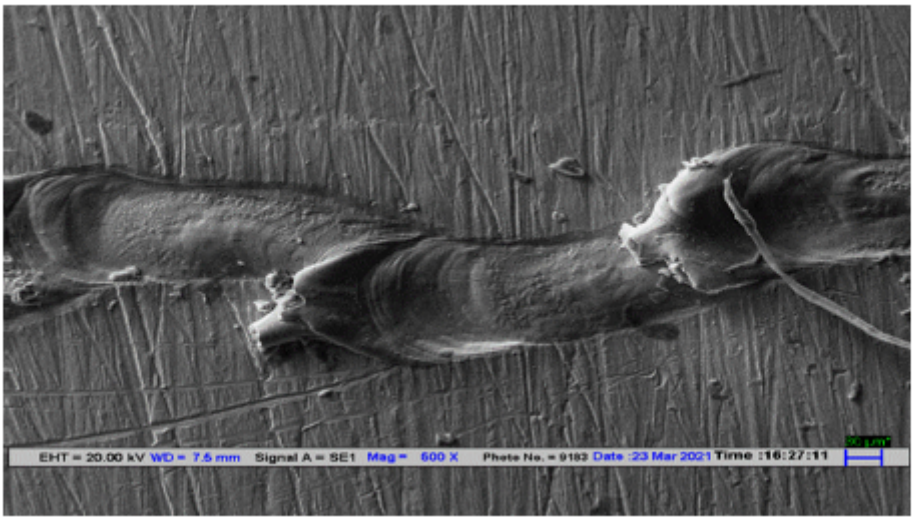

Figure 3

laser structured surface 20W

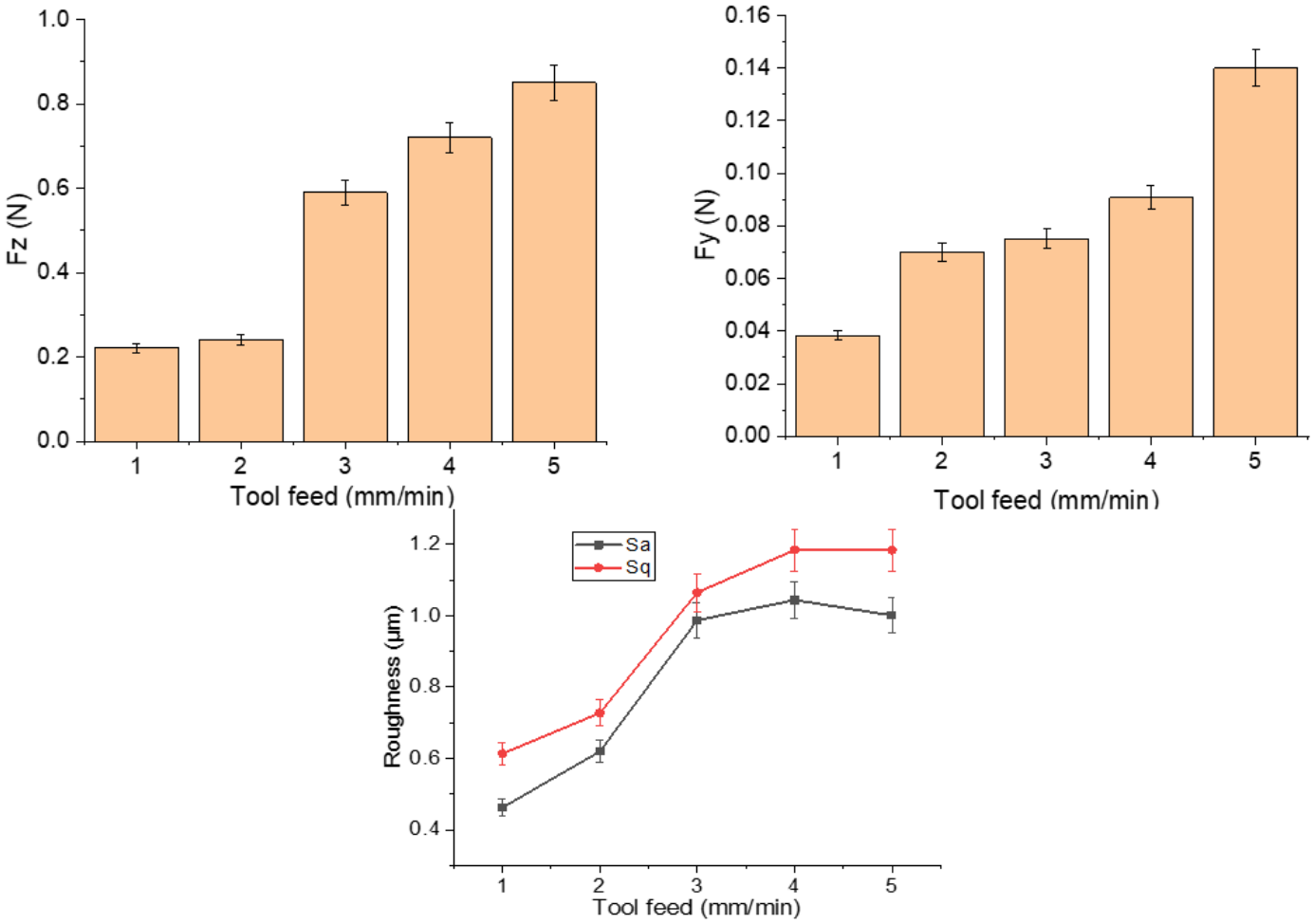

Figure 4

Effect of grinding feed on (a) Normal force (b)Tangential force (c) Roughness at vs=80mm/min, ap=5um

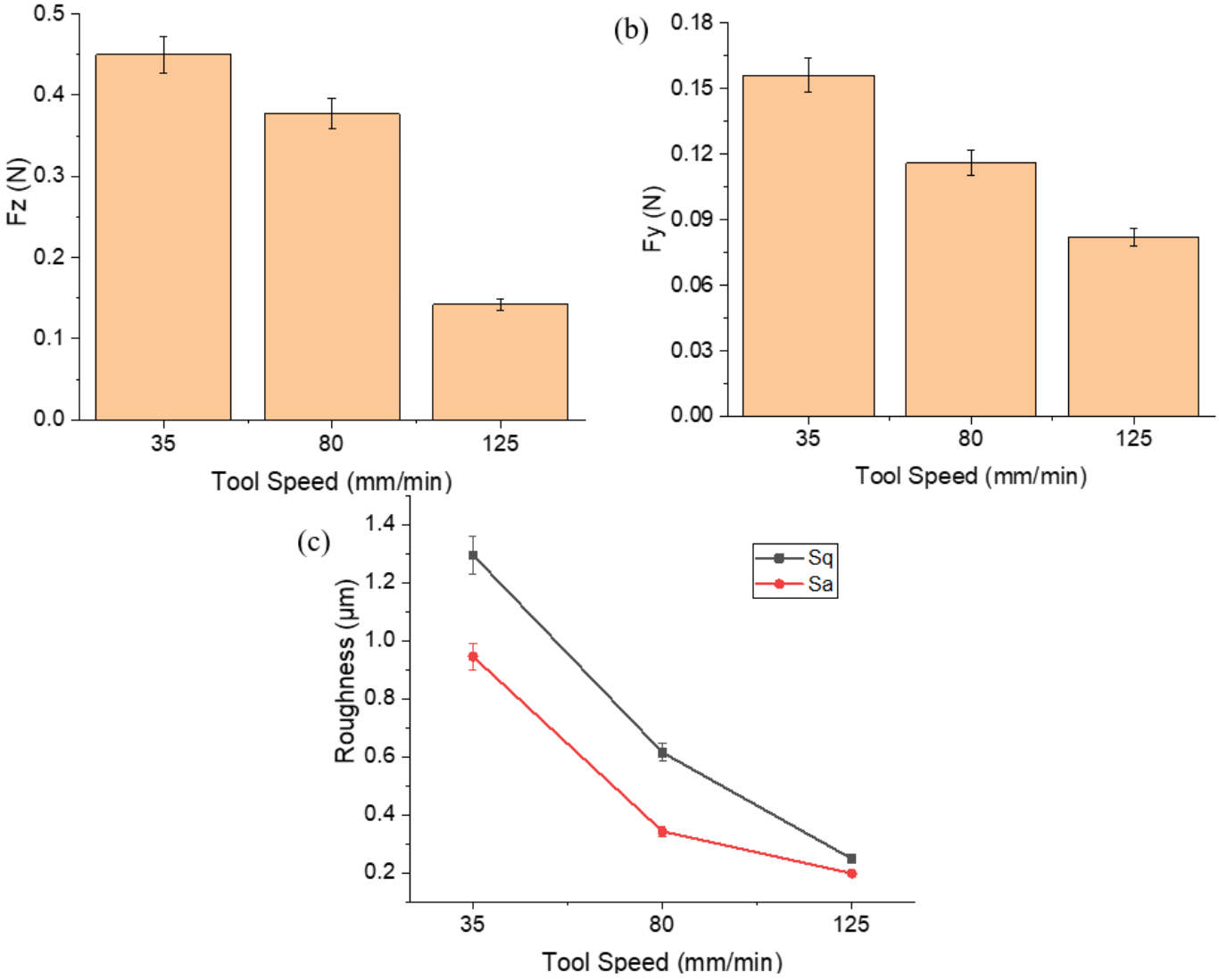

Figure 5

Effect of cutting speed (a) Normal force Fz (b)Tangential force(c)Roughness at f=1mm/min, ap=20μm

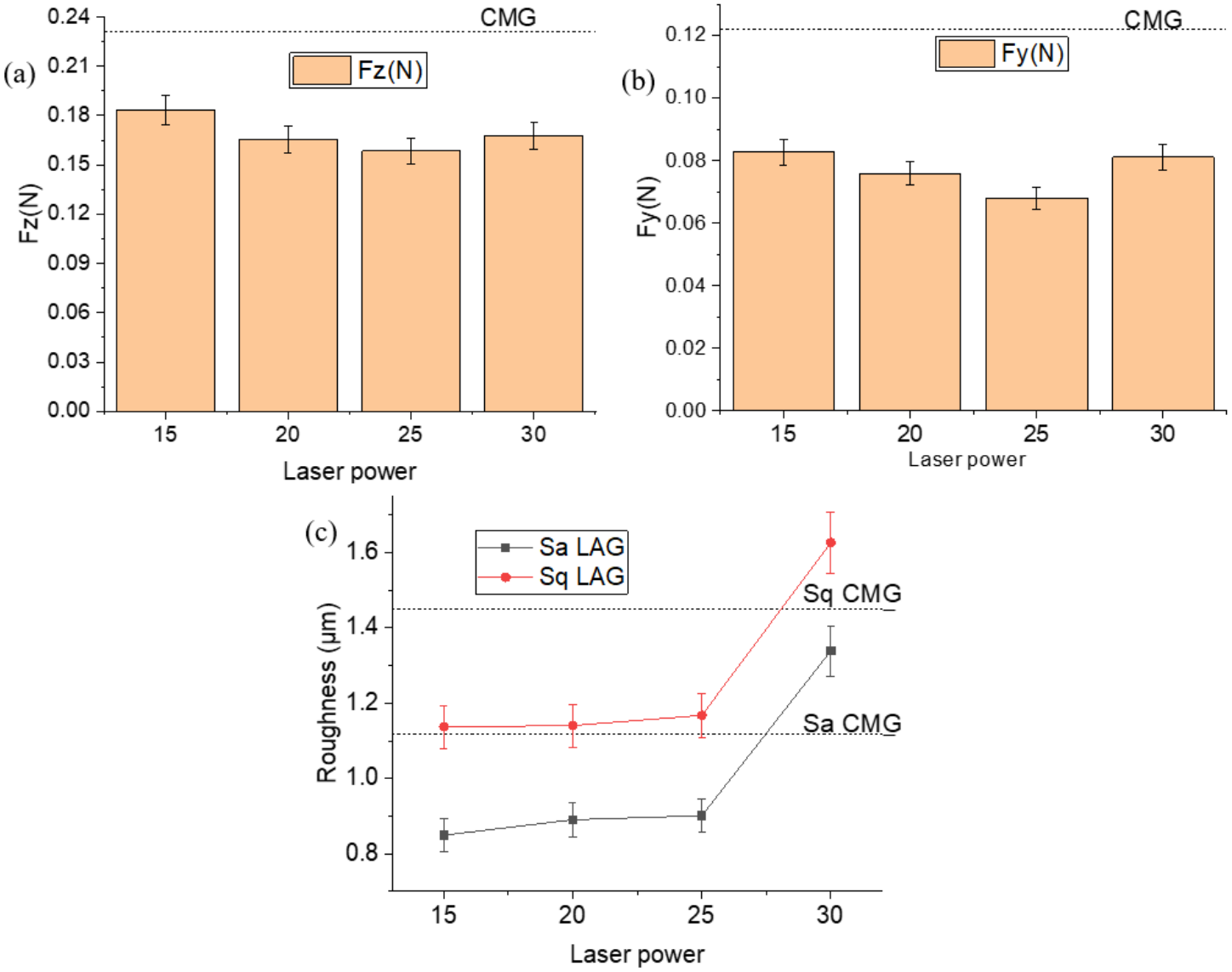

Figure 6

Effect of laser power with pattern 1 at tool f=2mm/min, ap=5μm and vs= 80mm/min. Fig 7 Effect of laser power on on (a) normal cutting force Fz (b)tangential cutting force Fy (c)Roughness

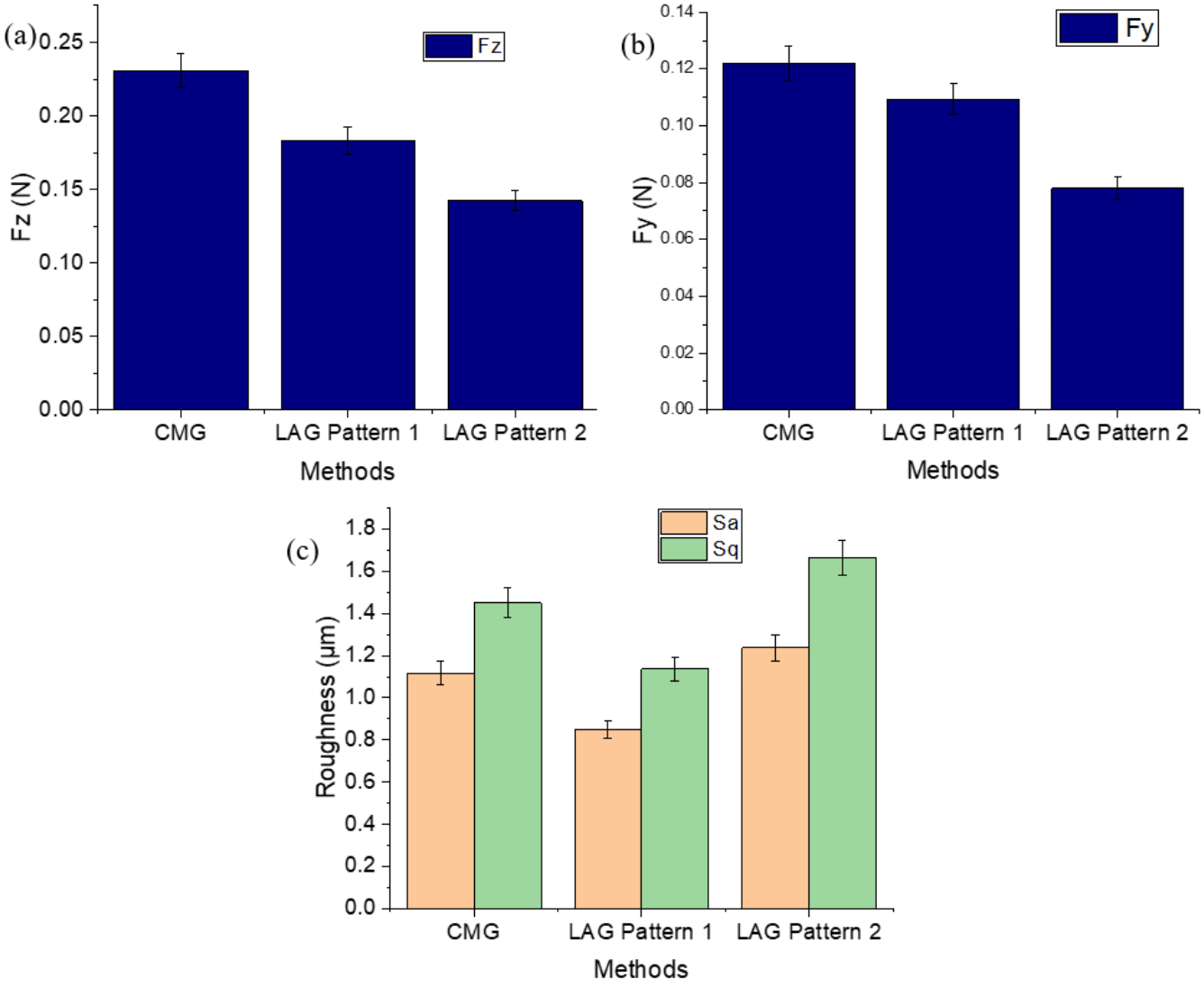

Figure 7

Effect of laser input energy density on pattern 1 and 2 at f=2mm/min, ap=5µm and vs= 80mm/min, Laser power 15W (a) Normal force (a) Tangential force and (c) Surface roughness

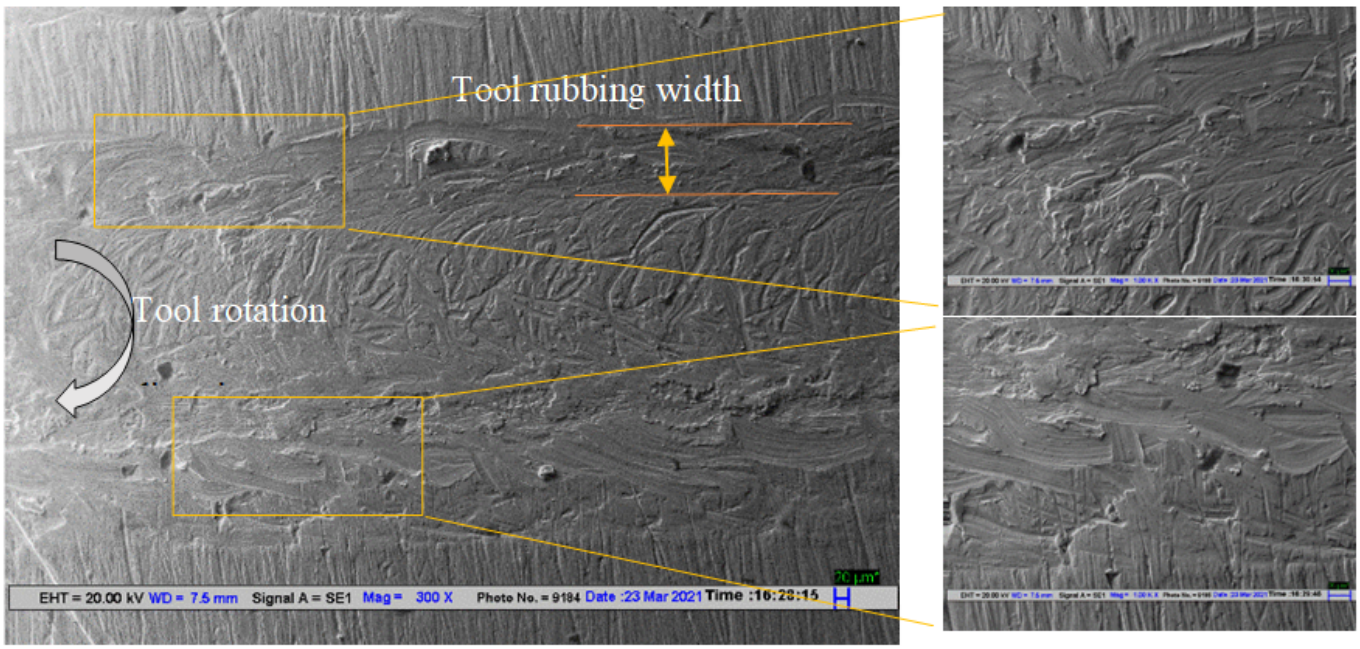

Figure 8

CMG process SEM micrograph vs=80mm/min, f=2 mm/min and ap=5μm.

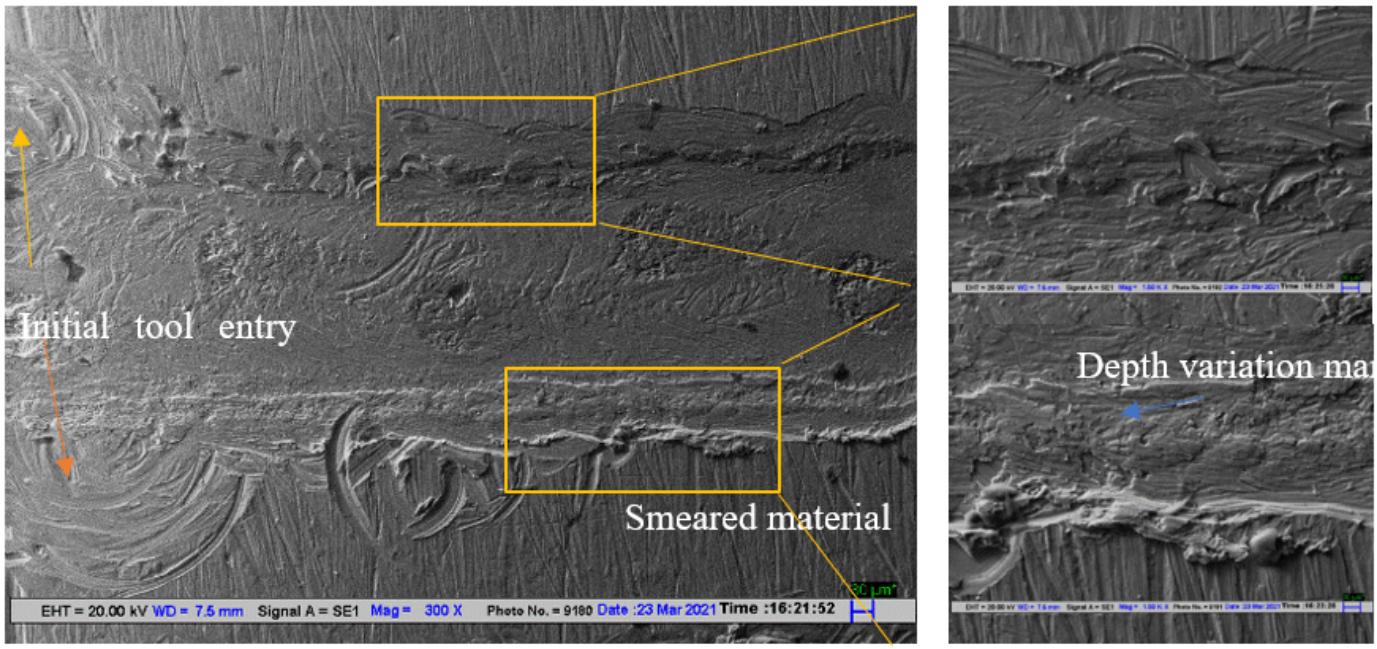

Figure 9

LAMG process SEM micrograph, Laser parameters: Pattern 1, P=15W 60mm/s; CMG paramters vs=80mm/min, f=2mm/min and ap =5μm

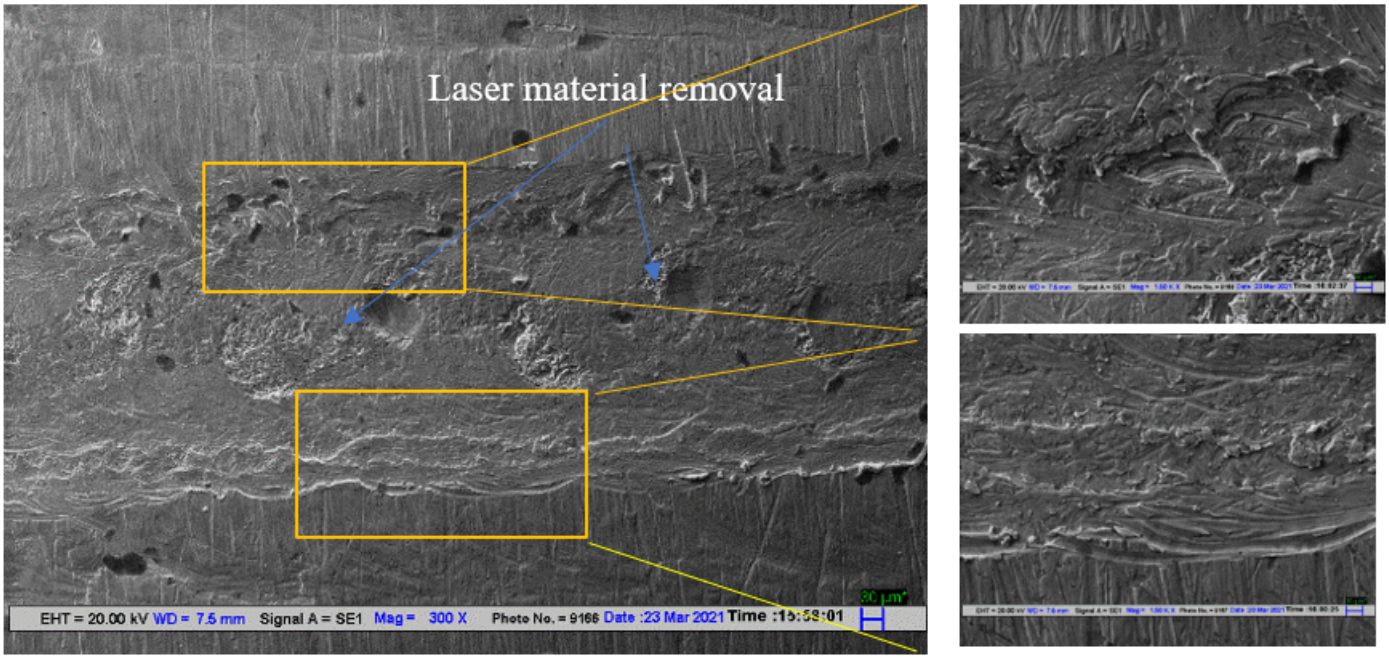

Figure 10

LAMG process SEM micrograph Pattern 2 Laser parameters P=15W 60mm/s; CMG paramters vs=80mm/min, f=2 mm/min and ap=5µm